Sphingolipids protect ergosterol in the *Leishmania major* membrane from sterol-binding toxins

Chaitanya S. Haram[1,4], Samrat Moitra[1,4], Rilee Keane[1], F. Matthew Kuhlmann[2], Cheryl Frankfater[3], Fong-Fu Hsu[3], Stephen M. Beverley[2], Kai Zhang[1], and Peter A. Keyel[1,*]

[1]Department of Biological Sciences
Texas Tech University
Lubbock, TX 79409

[2]Department of Molecular Microbiology
Washington University School of Medicine
St. Louis, MO 63110

[3]Mass Spectrometry Resource
Division of Endocrinology, Metabolism, and Lipid Research
Department of Medicine
Washington University School of Medicine
St. Louis, MO 63110

[4]These authors contributed equally

*to whom correspondence should be addressed
Peter Keyel
Department of Biological Sciences
Biology Rm 108
Box 43131
Lubbock, TX 79409-3131
tel: (806) 834-6248
fax: (806) 742-2963
email: peter.keyel@ttu.edu

Running Title: Sphingolipids protect *Leishmania*

Keywords: inositol phosphorylceramide; streptolysin O; perfringolysin O; pore-forming toxin; sterol

Abstract

Nephrotoxicity is one common side effect of the first line anti-leishmanial treatment, liposomal amphotericin B. Amphotericin B targets ergosterol, so one approach to reducing dose and side effects could be improving the access of the drug to its target. While the surface exposure of ergosterol in *Leishmania* is unknown, sterols in mammalian cells can be sheltered from sterol-binding agents by membrane components, including sphingolipids. Here, we tested the ability of the *Leishmania major* sphingolipids inositol phosphorylceramide (IPC), and ceramide to shelter ergosterol by preventing binding and cytotoxicity of the sterol-binding toxins streptolysin O and perfringolysin O using flow cytometry. In contrast to mammalian systems, *Leishmania* sphingolipids did not preclude toxin binding to sterols in the membrane. However, IPC interfered with cytotoxicity. Ceramide reduced perfringolysin O, but not streptolysin O, cytotoxicity in cells. Ceramide sensing was controlled by the toxin L3 loop. Ceramide was sufficient to protect *L. major* promastigotes from amphotericin B. These findings suggest that *L*. *major* offers a genetically tractable model organism for understanding toxin-membrane interactions. Furthermore, our findings suggest targeting ceramide may enhance the efficacy of ergosterol-targeting anti-leishmanial drugs.

Author Summary

Leishmaniasis is a neglected tropical disease with ~1.5-2 million new cases and ~70,000 deaths per year. One first-line treatment for leishmaniasis is liposomal amphotericin B, which is expensive and can damage the kidneys. One way to reduce cost and side effects is to reduce the needed dose by improving efficacy. In order to improve its efficacy, we need to learn how its target—ergosterol—is protected by other components of *Leishmania*. The human equivalent of ergosterol is protected by components called sphingolipids. We tested the ability of sphingolipids to protect ergosterol using pore-forming toxins. Pore-forming toxins need ergosterol to first bind and then kill *Leishmania*. Unlike human cells, toxins bound to ergosterol—indicating that they had access—even when sphingolipids were present. However, sphingolipids prevented the toxins from killing the cells, and provided protection from amphotericin B. These data reveal that *Leishmania* organizes its sterol-protective components differently from humans. Further, we can use toxins and *Leishmania* as a system to understand the fundamental rules governing how sterol-protecting components are organized in the membrane. We can then use this information to help improve liposomal amphotericin B efficacy.

Introduction

Annually, 1.5-2 million cases and 70,000 deaths are caused by the neglected tropical disease, leishmaniasis. One first-line treatment for leishmaniasis is liposomal amphotericin B, which binds to membrane ergosterol and induces pores in the membrane of the causative parasites in the genus *Leishmania* [1]. However, liposomal amphotericin B has strong nephrotoxic side-effects [2, 3], highlighting the need to develop new drug targets or to improve existing drugs by reducing the dose needed. One approach to improving amphotericin B efficacy is to enhance its access to ergosterol and ability to damage the membrane.

Membrane sterol access is primarily controlled by sphingolipids in mammalian cells. In mammalian cells, plasma membrane cholesterol is evenly split between sphingomyelin-cholesterol complexes, other “inaccessible” cholesterol, and “accessible” cholesterol [4]. Accessible cholesterol is defined by the ability of the membrane cholesterol to bind to exogenous sterol binding agents, like cholesterol-dependent cytolysins (CDCs) [4]. Sphingomyelinases liberate cholesterol from cholesterol-sphingomyelin complexes, increasing sterol sensitivity to CDCs [5]. Thus, sphingolipids govern the sterol accessibility in mammalian cells.

In comparison to mammalian cells, *Leishmania* synthesize different lipids, which could alter sterol accessibility. Like cholesterol, ergosterol forms detergent resistant microdomains with the primary *Leishmania* sphingolipid, inositol phosphorylceramide (IPC) and GPI-anchored proteins like gp63 [6]. IPC comprises 10% of the total lipids in *Leishmania major* [7], and is not recognized by the animal sphingolipid sensors Ostreolysin A or lysenin [8, 9]. IPC is not cleaved by *B. cereus* sphingomyelinase, and the lipase that cleaves IPC [10] likely cleaves other lipids, complicating the interpretation of any results. Two key enzymes affecting IPC are serine palmitoyl transferase (SPT), the first committed step of sphingolipid synthesis, and IPC

synthase (IPCS). Genetic ablation of the second subunit of SPT (*SPT2*) inactivates the enzyme. Knockout of *SPT2* prevents the formation of sphingosine, which leads to defects in ceramide and IPC synthesis and infectivity, but normal growth [6]. Similar results are observed when SPT2 is chemically inhibited with the drug myriocin [6]. Thus, both genetic and pharmacological tools exist to measure the control of *Leishmania* sphingolipids over ergosterol accessibility.

Sterol accessibility is measured using inactive cholesterol-binding cytolysins (CDCs) from Gram positive bacteria. Streptolysin O (SLO) and perfringolysin O (PFO), from *Streptococcus pyogenes* and *Clostridium perfringens* respectively, bind to cholesterol in the membrane, oligomerize and insert 20-30 nm pores into the membrane [11]. CDCs engage a range of sterols, including ergosterol [12]. One advantage of CDCs is that their properties can be changed using mutagenesis, which we and others have extensively characterized [13-19]. Binding can be ablated by mutating two residues that drive sterol recognition (ΔCRM), or by introducing mutations that interfere with glycan binding [18]. Similarly, mutation of two Gly to Val produce an inactive, non-toxic “monomer-locked” CDC that binds sterols [13, 15, 17]. Finally, SLO and PFO engage sterols in distinct, but unknown, lipid environments [14, 16]. SLO binds to and inserts into membranes faster than PFO [14, 16]. The increased rate of binding and insertion is interpreted as SLO binding in a wider range of sterol microenvironments than PFO [14, 16]. However, the identity of the microenvironment permissive for SLO or PFO remain unknown. The microenvironment requirements for each toxin can be switched to that of the other toxin by introducing point mutations in the membrane-binding L3 loop of the CDC [13, 14, 16]. Thus, CDCs represent a versatile tool for probing the membrane environment and accessibility of sterols.

Here, we tested the hypothesis that *Leishmania* shielded the ergosterol targets of amphotericin B in a manner similar to sterol shielding by mammalian cells. Surprisingly, we found that in

contrast to mammalian cells, *Leishmania* sphingolipids did not prevent CDC binding, yet were able to prevent CDC cytotoxicity. Ceramide more strongly reduced PFO cytotoxicity, suggesting ceramide is one determinant sensed by the L3 loop. Ceramide further contributed to the protection of *L. major* promastigotes from amphotericin B. Targeting ceramide and IPC may enhance ergosterol-targeting anti-leishmanial drugs.

Results

Sphingolipids do not limit accessible sterols in *L. major*

To determine if *L. major* sphingolipids shelter plasma membrane ergosterol, we measured the accessible ergosterol in wild type and sphingolipid-deficient *L. major* promastigotes. We used fluorescently labeled "monomer-locked" (ML) SLO and PFO, which detect accessible cholesterol in mammalian cells [19]. Both SLO ML and PFO ML exhibited dose dependent binding to wild type (WT) *L. major* (Fig 1A, B), indicating they can bind to ergosterol in the *Leishmania* plasma membrane. Surprisingly, the sphingolipid-null *spt2*$^{-}$ showed no increase in SLO or PFO ML binding (Fig 1A, B). Overexpression of SPT2 in the *spt2*$^{-}$ background (*spt2*$^{-}$ /+SPT2) also did not change CDC binding (Fig 1A, B). These data suggest that sphingolipids do not shelter ergosterol in *L. major*.

To confirm that sphingolipids do not shelter ergosterol in *L. major*, we used a *L. major* null mutant lacking the enzyme directly responsible for IPC synthesis from ceramide and phosphatidylinositol, *ipcs*$^{-}$. Knockout of *IPCS* eliminates IPC, but retains ceramide. To complement the knockout, episomal expression of IPCS in *ipcs*$^{-}$ cells (*ipcs*$^{-}$/+IPCS) was used. Similar to *spt2*$^{-}$, SLO ML and PFO ML binding of *ipcs*$^{-}$ was equivalent to wild type and *ipcs*$^{-}$ /+IPCS *L. major* (Fig 1C, D). Prior characterization of the *ipcs*$^{-}$ cells revealed an absence of IPC and accumulation of ceramide in the *ipcs*$^{-}$ cells, which was reverted by complementation [20]. We conclude that neither ceramide (absent in *spt2*$^{-}$) nor IPC (absent in both) alter ergosterol accessibility to CDCs in *L. major*.

While the CDCs can access ergosterol independently of sphingolipids, the amount of sterol and the extent of accessibility remains unclear. It was previously reported that *spt2*$^{-}$ *L. major* promastigotes have reduced ergosterol, but increased cholesterol levels [21]. To determine if interference in sphingolipid synthesis altered *L. major* sterol metabolism, we measured total

sterols from promastigotes by gas chromatography-mass spectrometry (GC-MS). Promastigotes with inactivated *de novo* sphingolipid synthesis had a statistically significant increase (30-100% more than WT control) in total sterols, but similar ergosterol and ergosterol isomer (like 5-dehydroepisterol) levels (Fig 1E). The sterol increase came from cholesterol (taken up from the media) and sterol biosynthetic intermediates (Fig 1E). To compare the CDC accessibility of sterols to mammalian cells, we challenged both HeLa cells and *L. major* promastigotes with fluorescent SLO ML. Compared to HeLa cells, promastigotes poorly bound to SLO (Fig 1F). We interpret the reduced binding to reflect low levels of accessible ergosterol, and/or the lower affinity of CDCs for ergosterol. Overall, these data suggest that CDCs sense ergosterol in *L. major* membrane independently of IPC or ceramide.

L. major sphingolipids limit CDC cytotoxicity

Since CDCs bind poorly to *L. major* regardless of the sphingolipid composition, we tested if the CDC binding was sufficient to promote cytotoxicity. We challenged log phase wild type, *spt2*$^{-}$ or *spt2*$^{-}$/+SPT2 promastigotes with SLO or PFO at 37ºC for 30 min. We found that SLO killed wild type *L. major* only at very high doses, but efficiently killed *spt2*$^{-}$ promastigotes (Fig 2A, Supplementary Fig S1, S2A). Although PFO did not kill wild type or *spt2*$^{-}$/+SPT2 promastigotes at any dose tested, it killed *spt2*$^{-}$ promastigotes like SLO (Fig 2B, Supplementary Fig S2B). We next tested the *ipcs*$^{-}$ and *ipcs*$^{-}$/+IPCS, and found that *ipcs*$^{-}$ behaved similarly to *spt2*$^{-}$ (Fig 2C, D, Supplementary Fig S2C, D). We determined the CDC concentration needed to kill 50% of the cells (LC_{50}) to compare the sensitivity of *spt2*$^{-}$ and *ipcs*$^{-}$ *L. major*, along with HeLa cells. We found that sphingolipid-deficient *L. major* were 1.5-2 times more resistant than HeLa cells when challenged with either SLO or PFO (Fig 2E, Supplementary Fig S2A-E). Since sphingolipid-deficient *L. major* had elevated cholesterol levels, it is possible the sterol intermediates mediate the cytotoxicity. We challenged *L. major* promastigotes deficient in sterol methyltransferase (*smt*$^{-}$), which have normal sphingolipids, but elevated cholesterol levels [22], with SLO. We

observed no killing of *smt*$^{-}$ *L. major* promastigotes at doses ≤32,000 HU/mL, despite equivalent binding of toxin (Supplementary Fig S2F, G). We conclude sterol alterations in sphingolipid-deficient *L. major* does not account for the observed cytotoxicity. Instead, sphingolipids protect *L. major* from CDC-mediated cytotoxicity.

To control for alternative mechanisms of membrane binding, any impurities in the CDC preparation, and the necessity of pore formation for *L. major* killing, we used three different non-hemolytic SLO mutants. The SLO ΔCRM lacks the cholesterol binding residues in domain 4 [18]. SLO Q476N cannot engage glycans on the cell surface needed for orientation [18, 23]. SLO ML binds normally, but cannot form pores [17, 19]. We challenged *spt2*$^{-}$ and *ipcs*$^{-}$ *L. major* with SLO ΔCRM, SLO Q476N, SLO ML or wild type SLO (Supplementary Fig S2A, C, H, I). While SLO WT killed both *spt2*$^{-}$ and *ipcs*$^{-}$ *L. major*, SLO ΔCRM, SLO Q476N, and SLO ML did not (Supplementary Fig S2A, C, H, I). Similarly, PFO ML failed to kill *spt2*$^{-}$ or *ipcs*$^{-}$ at all concentrations tested (Supplementary Fig S2B). These data indicate that *L. major* membranes engage the same binding determinants used by CDCs to target mammalian cells.

Since PFO and SLO showed different killing of wild type *L. major*, and have distinct membrane binding kinetics, we compared the rate at which SLO and PFO killed sphingolipid-deficient *L. major*. In mammalian cells, SLO more rapidly engages the membrane, whereas PFO binds more slowly [14]. Consequently, in HeLa cells there is a larger difference between PFO-mediated killing at 5 min and at 30 min than between SLO-mediated killing [13]. We tested the sensitivity of *spt2*$^{-}$ or *ipcs*$^{-}$ *L. major* after 5 min or 30 min of SLO or PFO challenge. For *spt2*$^{-}$, we found that both CDCs had significant changes in LC_{50} between 5 min and 30 min (Fig 2F, Supplementary Fig S2A, B, S3). While the SLO and PFO LC_{50} were similar at 30 min, at 5 min, there was a trend for less killing by PFO compared to SLO (Fig 2F). We next compared the *spt2*$^{-}$ and *ipcs*$^{-}$ mutants after CDC challenge. At 5 min, the *ipcs*$^{-}$ mutant was killed similarly to

spt2⁻ (Fig 2G, Supplementary Fig S3). These data indicate that sterol accessibility is insufficient to determine cytotoxic outcomes in *L. major*. Therefore, to sustain pore formation, SLO and PFO require different lipid environments in the *Leishmania* plasma membrane.

Growth phase of promastigotes does not alter CDC sensitivity

The lipid environment fluctuations during the *L. major* growth cycle could impact CDC sensitivity. The *spt2*⁻ promastigotes have defects in phosphatidylethanolamine (PE) synthesis when their growth reaches stationary phase [24]. In stationary phase, *L. major* promastigotes differentiate to the infectious metacyclic form over the course of approximately three days. We tested the impact of PE defects and metacyclogenesis on CDC killing of *spt2*⁻ *L. major*. We challenged *L. major* in log phase, or on day 1, 2 or 3 of stationary phase with 62-4000 HU/mL SLO or PFO. At the doses used, SLO and PFO killed *spt2*⁻ *L. major*, but did not kill wild type or *spt2*⁻/+SPT2 *L. major,* during stationary phase (Fig 3, Supplementary Fig S4A-F). The LC_{50} of SLO and PFO remained similar between log phase and throughout stationary phase (Figs 2-3), suggesting that changes in PE synthesis did not impact CDC killing of *L. major*. We next determined if the differences we observed for the SLO LC_{50} at 5 min and 30 min in log phase were also present during stationary phase. The SLO LC_{50} for stationary phase promastigotes changed similarly to log phase (Fig 3C, Supplementary Fig S4G-I). Overall, the sensitivity of *spt2*⁻ promastigotes to SLO and PFO did not significantly change during metacyclogenesis, suggesting that changes in PE during growth do not account for CDC sensitivity.

Ceramide hinders CDC cytotoxicity

One key difference between the *spt2*⁻ and *ipcs*⁻ that could account for the differences in cytotoxicity is ceramide. The *ipcs*⁻ accumulates ceramide because it cannot synthesize it into IPC, whereas the *spt2*⁻ cannot synthesize the precursors to ceramide. To determine the contribution of ceramide to CDC cytotoxicity, we used a chemical inhibitor of SPT, myriocin. We

treated wild type, *spt2*$^{-}$, *spt2*$^{-}$/+SPT2, *ipcs*$^{-}$, and *ipcs*$^{-}$/+IPCS promastigotes with myriocin prior to CDC challenge. Myriocin increased the SLO sensitivity of wild type and *ipcs*$^{-}$/+IPCS *L. major* similar to that of *spt2*$^{-}$, confirming inhibitor efficacy (Fig 4, Supplementary Fig S5A, B). While sensitized to CDCs, myriocin-treated *spt2*$^{-}$/+SPT2 were more resistant than myriocin-treated WT (Fig 4, Supplementary Fig S5). We attribute this resistance to elevated SPT2 levels in these promastigotes [6]. There was no change in the SLO LC_{50} for *spt2*$^{-}$ after myriocin treatment, indicating that myriocin was specific for SPT in our assay (Fig 4). However, the LC_{50} for *ipcs*$^{-}$ *L. major* decreased 2-fold for SLO and 6-fold for PFO upon myriocin treatment (Fig 4, Supplementary Fig S5). Furthermore, this increase in sensitivity surpassed that of either *spt2*$^{-}$ or *ipcs*$^{-}$ alone (Fig 4, Supplementary Fig S5). We interpret this finding to indicate that ceramide, which accumulates in *ipcs*$^{-}$, but not *spt2*$^{-}$ promastigotes, contributes to protecting the *Leishmania* membrane from damage. Thus, ceramide and other perturbations in the lipid environment might contribute to protection from PFO.

Since PFO showed larger differences in *ipcs*$^{-}$ *and spt2*$^{-}$ with and without myriocin, we interpret these findings to indicate that PFO is more sensitive to the overall lipid environment in the membrane than SLO. To test this interpretation, we challenged myriocin-treated, *I*nositol phospho*S*phingolipid phospholipase *C*-*L*ike (ISCL)-deficient (*iscl*$^{-}$) *L. major* with CDCs. *iscl*$^{-}$ *L. major* lack the lipase that converts IPC back into ceramide, and have elevated IPC levels [10]. In contrast to myriocin-treated *ipcs*$^{-}$ *L. major*, which contain low levels of ceramide, myriocin-treated *iscl*$^{-}$ *L. major* contain low levels of IPC. When challenged with SLO or PFO, myriocin-treated *iscl*$^{-}$ promastigotes phenocopied myriocin-treated WT promastigotes (Fig 4C, D, Supplementary Fig S5C, D). Consistent with the primary role of IPC in conferring resistance to cytotoxicity, untreated *iscl*$^{-}$ or *iscl*$^{-}$/+ISCL *L. major* were resistant to SLO and PFO challenge, even at high toxin doses (Fig 4C, D, Supplementary Fig S5C, D). Notably, myriocin-treated *ipcs*$^{-}$ promastigotes were more sensitive to CDCs compared to WT or *iscl*$^{-}$ promastigotes (Fig

4C, D, Supplementary Fig S5C, D). Overall, these data suggest that IPC provides the most protection against cytotoxicity, but ceramide also protects *L. major* from the cytotoxicity of pore-forming toxins.

The L3 loop in CDCs senses ceramide in the plasma membrane

We next determined the mechanism by which PFO is more sensitive to ceramide. One key difference between the membrane binding and accessibility of SLO and PFO is the amino acid sequence of the L3 loop [14, 16]. These differences in L3 loop can be switched by single point mutations. SLO S505D confers PFO-like binding and cytotoxicity on SLO, while PFO D434K has SLO-like binding and cytotoxicity [13, 14, 16]. We tested if the cytotoxic differences we observed between CDCs— killing of wild type *L. major* at high toxin concentrations and the differences in *spt2*$^{-}$ and *ipcs*$^{-}$ LC_{50}— could be explained by these L3 loop differences. We challenged wild type, *spt2*$^{-}$, *ipcs*$^{-}$ and add-back *L. major* promastigotes with PFO, PFO D434K, SLO or SLO S505D for 30 min. We found that PFO D434K killed wild type and *spt2*$^{-}$/+SPT2 *L. major* at high concentrations, similar to SLO, while PFO did not kill wild type *L. major* or the *spt2*$^{-}$/+SPT2 (Fig 5A, B). SLO S505D phenocopied PFO, failing to kill wild type or *spt2*$^{-}$/+SPT2 *L. major* (Fig 5A, B). While both PFO and PFO D434K killed *spt2*$^{-}$ *L. major*, SLO S505D was less effective than either PFO or SLO in killing *spt2*$^{-}$ *L. major* (Fig 5A, B). This is consistent with our previous findings in mammalian cells that SLO S505D has a higher LC_{50} than wild type SLO or PFO [13]. We repeated these experiments using *ipcs*$^{-}$ *L. major*. We found broadly similar results with *ipcs*$^{-}$ (Fig 5C, D). We were able to calculate LC_{50} values for wild type *L. major* and *ipcs*$^{-}$/+IPCS with SLO and PFO D434K only (Fig 5E). We conclude that the differences in SLO and PFO cytotoxicity are due to differential sensing of ceramide by the L3 loop.

Ceramide and IPC protect *L. major* promastigotes from amphotericin B

Finally, these findings suggest that sphingolipid-deficient *L. major* promastigotes are more sensitive to amphotericin B. We first titrated both myriocin and amphotericin B against WT *L. major* promastigotes to determine the EC_{50}. We found the EC_{50} of amphotericin B was 30 nM, while myriocin did not inhibit growth more than 25% promastigotes at 10 μM. This is similar to the published EC_{50} of amphotericin B, which is 33 nM [25]. We next challenged log phase myriocin-treated WT and untreated WT, *spt2*$^{-}$, *spt2*$^{-}$/+*SPT2*, *ipcs*$^{-}$, *ipcs*$^{-}$/+*IPCS* promastigotes with amphotericin B. Removal of both IPC and ceramide increased the sensitivity of *L. major* 2-3-fold, whereas loss of only IPC was not sufficient to increase sensitivity to amphotericin B (Fig 6). We conclude that both ceramide and IPC are needed to protect *L. major* promastigotes from amphotericin B.

Based on these data, we propose a new model of CDC engagement with the *Leishmania* membrane. CDCs are able to bind to the membrane, independently of sphingolipids (Fig 7). In the absence of sphingolipids, both SLO and PFO oligomerize and insert into the membrane to kill the cell (Fig 7). The presence of ceramide without IPC provides limited protection against PFO, but not SLO. Recognition of ceramide in this environment is controlled by the L3 loop. Similarly, when Leishmania have their full complement of sphingolipids, ceramide precludes PFO toxicity at high doses, but not SLO (Fig 7). At lower toxin concentrations, however, the sphingolipids prevent toxin insertion by both CDCs.

Discussion

Here we used the human pathogen *L. major* as a medically relevant model organism to understand toxin-membrane interactions. In contrast to mammalian systems, we found that *Leishmania* sphingolipids do not preclude CDC binding to sterols in the membrane, yet still interfere with cytotoxicity. Interference in toxicity was predominantly due to IPC. We further identified ceramide as one lipid that selectively reduces PFO, but not SLO, cytotoxicity in cells. Disruption of both IPC and ceramide increased sensitivity of *L. major* to the anti-*Leishmania* drug amphotericin B. These data show that IPC and ceramide protect *L. major* from ergosterol-binding, pore-forming toxins.

In *L. major*, sphingolipids limited CDC cytotoxicity without reducing binding. There are several potential reasons why CDCs show equivalent, low levels of binding to *L. major* membranes independently of sphingolipids. One key reason may be ergosterol. While ergosterol retains the key sterol binding elements—the 3β-OH group, double bond at C5 and C6 carbon atoms of B ring and an iso-octyl side chain—needed for PFO engagement [26], it binds more poorly to CDCs than cholesterol does [26]. Alternatively low CDC binding may occur because ergosterol associates with other phospholipid molecules such as phosphatidylcholine (PC), phosphatidylethanolamine (PE) and phosphatidylserine (PS) in the *Leishmania* plasma membrane [6]. The glycoprotein gp63 prevents Complement-mediated lysis [27]. However, gp63 is unlikely to shelter ergosterol in *L. major* promastigotes. First, SLO and PFO engage glycoproteins on the mammalian cell surface [18, 23]. Secondly, eliminating the ability of SLO to engage glycoproteins removed its ability to kill *spt2*$^{-}$ *L. major*. Finally, *spt2*$^{-}$ promastigotes have wild type levels of lipophosphoglycan and gp63 [6], yet were robustly killed by SLO and PFO. We interpret these findings to indicate that glycoproteins do not shelter ergosterol. The failure of SLO ΔCRM to kill *L. major* suggests that CDCs engage ergosterol in the leishmania membrane.

Ergosterol may not be sheltered due to structural differences between sphingomyelin and IPC. Based on the crystal structure of the sphingomyelin/cholesterol-binding Ostreolysin A and docking models with sphingomyelin, the choline headgroup flexibly lies across the membrane when sphingomyelin is complexed with cholesterol [28]. In contrast, the inositol headgroup of IPC is unlikely to adopt this conformation. This could account for the inability of IPC to prevent CDC binding to ergosterol.

We also considered the possibility that sphingolipid perturbations altered sterols, and altered sterols were responsible for the observed phenotypes. A previous study [21] reported that *spt2*$^{-}$ promastigotes have lower ergosterol levels, and higher cholesterol levels. While we confirmed an increase in cholesterol and other sterol species with both genetic and chemical inhibition of SPT, we suggest this increase did not impact CDC binding or cytotoxicity. We observed no difference in CDC binding, suggesting that any sterol level alterations were insufficient to change CDC binding to the membrane. Since cholesterol is also involved in pore-formation [29], we tested *L. major* promastigotes lacking SMT [22]. The *smt*$^{-}$ have elevated total sterols, and accumulation of cholesterol-type sterols, yet were not killed by SLO. Based on these considerations, we conclude that IPC and ceramide are primary determinants for CDC cytotoxicity, but not binding, to Leishmania membranes.

The failure to prevent binding by CDCs may represent different physiologic needs of *L. major* and mammalian cells. Mammalian cells need to sense sterol levels provided exogenously by the organism to modify sterol synthesis [4], promote cellular signalling, and endocytosis [30-32]. In contrast, *Leishmania* promastigotes are free swimming organisms dependent on synthesizing their own sterols. Furthermore, no clear homologues of the sterol synthesis regulators sterol regulatory element-binding proteins (SREBP) or SREBP cleavage-activating protein (SCAP) have been detected in *Leishmania*. The lack of complications from SREBP signalling represents

one advantage to using *Leishmania* as a model organism to understand sterol membrane dynamics.

We focused on promastigotes *in vitro* because they synthesize lipids *de novo*. The transition from log phase promastigotes to the infectious metacyclic form did not adversely impact CDC toxicity. Importantly, *spt2*$^{-}$ promastigotes are unable to synthesize ethanolamine and thus have defects in phosphatidylethanolamine (PE) synthesis in stationary phase [24]. However it remains to be seen if PE synthesis plays a role in affecting CDC cytotoxicity. It remains to be determined what impact other phospholipids have on cytotoxicity in *L. major*. In mammalian cells, phospholipids regulate cholesterol access [33]. We did not examine amastigotes because they salvage lipids from the host macrophage [34-36], the membranes are substantially similar in *spt2*$^{-}$, *ipcs*$^{-}$, and wild type amastigotes [20, 37], and contaminating macrophage membranes could obscure results.

While changes in *Leishmania* sphingolipid status did not interfere with CDC binding, changes in both IPC and ceramide reduced the ability of CDCs to kill *L. major*. This finding adds to the controversial role of sphingomyelin and ceramide in preventing vs accentuating damage in mammalian cells. On one hand, the sphingomyelinase/pore-forming toxin combination is evolutionarily conserved from bacteria like *C. perfringens* up to venoms in bees and snakes, suggesting that destroying sphingomyelin enhances toxicity. On the other hand, acid sphingomyelinase [38] and/or neutral sphingomyelinase [5] have been reported to promote membrane repair. In mammals, it is not possible to separate the effects of sphingomyelin on cholesterol accessibility from the effects of sphingomyelin on directly interfering with CDC pore formation. Since IPC does not shelter sterol, we were able to determine that IPC interferes with pore formation. This suggests that sphingolipids comprise one key component of the non-permissive membrane environment that reduces CDC pore-formation.

We used differences in SLO and PFO binding to further probe the non-permissive environment. SLO binds more rapidly to membranes, whereas PFO requires more time to reach a permissive membrane environment [14]. This time difference is reflected in kinetic differences for PFO, but not SLO, cytotoxicity [13]. Like mammalian cells, we observed kinetic differences in CDC cytotoxicity in *L. major*. Importantly, PFO was unable to find an environment to promote pore formation in *L. major*, even at supraphysiologic doses. This phenotype was reversed by point mutations in the L3 loop that switch the membrane specificity between PFO and SLO. Since PFO D434K regained the ability to kill wild type *L. major*, we conclude that this part of the L3 loop discriminates IPC and/or ceramide. Our findings are consistent with the idea that the L3 loop is important not just for membrane binding, but also for controlling the lipid environment needed to sustain pore formation [14]. Whether the L3 loop also discriminates sphingomyelin in mammalian cells remains to be determined. Future work is also needed to determine the stage (oligomerization vs pore insertion) at which sphingolipids arrest cytotoxicity. Since Complement-mediated lysis relies on lipophosphoglycan [39], future work is further needed to determine if sphingolipids protect *L. major* from other toxins and Complement-mediated lysis during infection.

Ceramide may modulate CDC cytotoxicity in *L. major*. We found significant differences between the extent of cytotoxicity in the *spt2*$^{-}$ and *ipcs*$^{-}$, both of which lack IPC. We found that this difference was more pronounced when we blocked SPT with myriocin in the *ipcs*$^{-}$, even though myriocin treatment phenocopied the *spt2*$^{-}$ in our system. The key difference in IPC blockade is that SPT is upstream of ceramide synthesis, whereas IPCS is downstream of ceramide. We also combined myriocin treatment with ISCL, which catalyzes the opposite reaction compared to IPCS. Loss of both IPC and ceramide would prevent both IPC synthesis and ceramide accumulation, which led to increased cytotoxicity. This suggests that IPC is more protective than

ceramide, but ceramide also enhances protection. This contrasts with findings that addition of ceramide to liposomes containing 35% cholesterol increased membrane permeability to SLO [40]. The differences may be due to the system used, though we cannot rule out that ceramide mediates protection via a ceramide-lipid/protein complex, or that loss of ceramide causes changes in membrane fluidity that permit the sensing of other lipid species. One argument against fluidity changes is that the proportion of detergent resistant membranes is not changed in *spt2*$^{-}$ *L. major* [6]. Alternatively, ceramide may only be relevant when IPC is absent. In mammalian cells, ceramide homeostasis is crucial for apoptosis, with any dysregulation causing cell death [41], and ceramide accumulation was proposed as one potential switch mediating CDC cytotoxicity [42]. However, it is unclear if this process is conserved in *Leishmania*. Overall, this suggests that ceramide is one lipid species sensed by CDCs when forming pores in membranes.

While we showed that *Leishmania* sphingolipids limit cytotoxicity, but not binding, our study had limitations that can be explored in future studies. We did not determine the total fraction of plasma membrane ergosterol needed to support lysis by CDCs. In mammals, binding of inactive CDCs were used to probe the proportion of cholesterol [4]. However, our binding studies suggest that in *L. major*, this approach would underestimate the amount of membrane ergosterol that supports CDC-mediated lysis. We did not use a mouse model. The high efficacy of the single agents in the mouse model makes detecting synergistic effects from combination therapy there challenging.

Material and Methods

*Reagent*s All reagents were from Thermofisher Scientific (Waltham, MA, USA), unless otherwise noted. Cysteine-less His-tagged PFO (PFO WT) in pET22 was a generous gift from Rodney Tweten (University of Oklahoma Health Sciences Center, Oklahoma City, OK, USA). Cysteine-less, codon-optimized SLO (SLO WT) in pBAD-gIII was synthesized at Genewiz (New Brunswick, NJ). The C530A mutant retains wildtype binding, hemolytic activity and pore structure, but it is redox resistant [43]. Monomer-locked (G398V/G399V) SLO, cysteine-less SLO (C530A) , SLO S505D and PFO D434K were previously described [13, 19]. Glycan-binding (SLO Q476N) [18], and cholesterol binding (SLO T564A/L565A) (SLO ΔCRM) SLO mutants [44], and monomer-locked (G298V/G299V) PFO mutants were generated using Quikchange PCR and verified by Sanger sequencing. Primer sequences are available upon request.

Recombinant Toxins Toxins were induced and purified as previously described [19, 45]. Toxins were induced with 0.2% arabinose (SLO WT, SLO S505D, SLO G398V/G399V, SLO Q476N, SLO T564A/L565A (ΔCRM)), or 0.2 mM IPTG (PFO, PFO D434K, and PFO G298V/G299V) for 3 h at room temperature and purified using Nickel-NTA beads. For Cy5 conjugation, recombinant toxins were gel filtered into 100 mM sodium bicarbonate (pH 8.5) using a Zeba gel filtration column according to manufacturer's instructions. Enough Cy5 monoreactive dye (GE Healthcare) to label 1 mg protein was added to 3-4 mg toxin and incubated overnight at 4°C. Conjugated toxins were gel filtered into PBS to remove unconjugated Cy5 dye, aliquoted, and snap-frozen in dry ice. Protein concentration was determined by Bradford assay and hemolytic activity was determined as previously described [13] using human red blood cells (Zen Bio, Research Triangle Park, NC, USA). One hemolytic unit is defined as the amount of toxin required to lyse 50% of a 2% human red blood cell solution in 30 min at 37 °C in 2 mM $CaCl_2$, 10 mM HEPES, pH 7.4, and 0.3% BSA in PBS. The specific activities of SLO monomer-locked Cy5 and PFO monomer-locked Cy5 were <10 HU/mg. They were used at a mass equivalent to

wild-type SLO and PFO. Multiple toxin preparations were used (Table 1).

Table 1. Specific activity of active toxin preps used

Toxin	Figure Used	Specific Activity (HU/mg)
SLO WT	2A, 2C, 2E, S2C	1.23×10^6
	2E, S2A, S2E	8.3×10^4
	2F, 2G, S3	1.42×10^5
	3B, S4D-F	3.4×10^5
	3C, S4G-I	1.11×10^5
	4, S5	3.3×10^5
	5	3.3×10^5
	S1	4.92×10^5
	S2G	3.77×10^5
	S2H-I	2×10^5
SLO S505D	5	3.95×10^4
PFO D434K	5	7.87×10^6
PFO WT	2B, 2D, S2D	8.39×10^6
	2F, S2B, S2E	2.73×10^4
	2F, S3	1.92×10^6
	2E	1.63×10^5
	2G, S3, 4, S5	3.63×10^5
	3, S4	4.57×10^6
	5	1.75×10^6

Leishmania strains and culture LV39 clone 5 (Rho/SU/59/P) was used as the wild type strain, and all genetic mutants were made in this background. The serine palmitoyltransferase subunit 2 knockout Δspt2::HYG/Δspt2::PAC (*spt2*$^-$), episomal addback Δspt2::HYG/Δspt2:PAC/+pXG-SPT2 (*spt2*$^-$/+SPT2) [6], the inositol phosphosphingolipid phospholipase C-like knockout Δiscl2::HYG/Δiscl2::PAC (*iscl*$^-$), episomal addback Δiscl2::HYG/Δiscl2::PAC/+pXG-ISCL (*iscl*$^-$/+ISCL) [46], sterol methyltransferase knockout Δsmt::HYG/Δsmt::PAC (*smt*$^-$) [22], and episomal addback Δsmt::HYG/Δsmt::PAC/+pXG-SMT (*smt*$^-$/+SMT)[22] have been previously described. The inositol phosphorylceramide synthase knockout Δipcs::HYG/Δipcs::PAC (*ipcs*$^-$) and episomal addback Δipcs::HYG/Δipcs::PAC /+pXG-IPCS (*ipcs*$^-$/+IPCS) were generated in the Beverley lab [20]. Elevation of ceramide levels and lack of IPC were confirmed by mass spectrometry [20]. Wild type *L. major* LV39, *spt2*$^-$, *ipcs*$^-$, *smt*$^-$ and *iscl*$^-$ were cultured at 27°C in M199 medium with 0.182% $NaHCO_3$, 40 mM Hepes, pH 7.4, 0.1 M adenine, 1 μg/mL biotin, 5

μg/mL hemin & 2 μg/mL biopterin and 10% heat inactivated fetal bovine serum (FBS), pH 7.4. Episomal addback cells *spt2*$^{-}$/+SPT2, *ipcs*$^{-}$/+IPCS, *smt*$^{-}$/+SMT, and *iscl*$^{-}$/+ISCL were maintained in complete medium in the presence of 10 μg/mL neomycin (G418) and 20 μg/mL blasticidin (BSD), except experimental passages.

Culture density and cell viability were determined by hemocytometer counting and flow cytometry after propidium iodide (PI) staining at a final concentration of 20 μg/mL. In this study, log phase promastigotes refer to replicative parasites at 2.0 – 8.0 x10^6 cells/mL, and stationary phase promastigotes referred to non-replicative parasites at densities higher than 2.0 x10^7 cells/mL. Cells are considered Stationary Day 0 when they reach 2.0 x10^7 cells/mL. They are Stationary Day 1, Stationary Day 2 and Stationary Day 3 at 24, 48, 72 hours after they reach Stationary Day 0, respectively.

Drug treatment of L. major For myriocin treatment experiments, experimental log phase cells were seeded at 1.0 x10^5 cells/mL in complete medium and either treated with 10 μM Myriocin dissolved in 1X DMSO (experimental) or an equivalent volume of diluent 1x DMSO (control). Cells were cultured and allowed to reach log phase in 48 hours before harvesting and processing cells for experiments. For amphotericin B, log phase *L. major* promastigotes were inoculated in complete M199 media at 2.0 × 10^5 cells/ml in 0–100 nM of amphotericin B. Culture densities were measured after 48 hours of incubation in 24-well plates. EC_{50} and EC_{25} were determined by logistic regression using cells grown in the absence of amphotericin B as controls.

Leishmania processing for experiments Cells were cultured in complete medium to log phase or stationary phase, according to experimental requirements. Cells were counted, centrifuged at 3200 RPM (Rotor SX4750), 8 min to pellet cells at room temperature (25°C). Cells were washed

with 1X PBS and counted again for accuracy. Cells were centrifuged at 3200 RPM (Rotor SX4750), 8 min to pellet cells at room temperature (25°C), and resuspended in serum free 1X M199 to a final concentration of 1.0 x10^6 cells/mL. Thus, 100 µL of cells used per sample / well in 96 well plates contained 1.0 x10^5 cells.

HeLa cell culture Hela cells (ATCC (Manassas, VA, USA) CCL-2) were maintained at 37°C, 5% CO_2 in DMEM (Corning, Corning, NY, USA) supplemented with 10% Equafetal bovine serum (Atlas Biologicals, Fort Collins, CO, USA) and 1× L-glutamine (D10). They were negative for mycoplasma by microscopy.

Binding assay with L. major promastigotes L. major promastigotes were resuspended at 1 x10^6 cells/mL in M199 media supplemented with 2 mM $CaCl_2$ and 20 µg/mL propidium iodide. Cy5-conjugated toxins were diluted in serum free M199 media according to a mass equivalent to active toxin and further diluted in two-fold intervals. Cells were examined for PI and Cy5 fluorescence using an Attune flow cytometer. Debris was gated out and cells exhibiting high PI fluorescence (1-2 log shift) (PI high), low PI fluorescence (~1 log shift) (PI low) or background PI fluorescence (PI neg) were quantified, normalized against untreated cells and graphed according to mass used for inactive toxin (Supplemental Fig S1). Both PI neg and PI low populations remain metabolically active, indicating that only the PI high population are dead cells [47]. The median fluorescence intensity (MFI) of Cy5 labeled, PI negative population was quantified, background-subtracted using cells receiving no Cy5-conjugated toxin. MFI was plotted against mass of inactive Cy5-conjugated toxin (SLO ML or PFO ML).

Cytotoxicity assay with Leishmania major promastigotes L. major promastigotes were resuspended at 1 x10^6 cells/mL in M199 media supplemented with 2 mM $CaCl_2$ and 20 µg/mL propidium iodide. HeLa cells were resuspended at 1x 10^6 cells/mL in RPMI media supplemented

with 2 mM $CaCl_2$ and 20 µg/mL propidium iodide. Toxins were diluted in serum free M199 media for *Leishmania* promastigotes or in serum free RPMI media for Hela cells according to hemolytic activity (wild-type toxins) or equivalent mass (inactive mutant toxins) and further diluted in two-fold intervals. PI fluorescence in cells was measured using an Attune flow cytometer. Debris was gated out and cells exhibiting high PI fluorescence (1-2 log shift) (PI high), low PI fluorescence (~1 log shift) (PI low) or background PI fluorescence (PI neg) were quantified, normalized against untreated cells and graphed according to toxin concentration (Supplemental Fig S1). Specific lysis was determined as follows: % Specific Lysis = (% PI $High^{Experimental}$ - % PI $High^{Control}$) / (100 - %PI $High^{Control}$). The sublytic dose was defined as the highest toxin concentration that gave <20% specific lysis.

Sterol analysis by gas chromatography/mass spectrophotometry (GC-MS). Total lipids were extracted according to a modified Folch's protocol [48]. *L. major* promastigotes (DMSO treated or treated with 10 µM myriocin for 48 h first) were resuspended in chloroform: methanol (2:1) at 1.0×10^8 cells/mL along with the internal standard cholesta-3,5-diene [(FW=368.84) from Avanti Polar Lipids] at 2.0×10^7 molecules/cell and vortexed for 30 seconds. Cell debris was removed by centrifugation (2500 RPM/1000 g for 10 minutes) and supernatant was washed with 0.2 volume of 1X PBS. After centrifugation, the aqueous layer was removed and the organic phase was dried under a stream of N_2 gas. Lipid samples were then dissolved in methanol at the equivalence of 1.0×10^9 cells/mL. An internal standard, cholesta-3,5-diene (formula weight, 368.34), was provided at 2.0×10^7 molecules/cell during extraction. For GC-MS, equal amounts of lipid extract were transferred to separate vial inserts, evaporated to dryness under nitrogen, and derivatized with 50 µL of N,O-Bis(trimethylsilyl)trifluoroacetamide plus 1% trimethylchlorosilane in acetonitrile (1:3), followed by heating at 70°C for 30 min. GC-MS analysis was conducted on an Agilent 7890A GC coupled with Agilent 5975C MSD in electron ionization mode. Derivatized samples (2 µL each) were injected with a 10:1 split into the GC

column with the injector and transfer line temperatures set at 250 °C. The GC temperature started at 180°C and was held for 2 min, followed by 10°C/min increase until 300°C and then held for 15 min. To confirm that the unknown GC peak retention time matched that of the episterol standard, we also used a second temperature program started at 80°C for 2 min, ramped to 260 °C at 50°C/min, held for 15 min, and increased to 300°C at 10°C/min and held for 10 min. A 25-m Agilent J & W capillary column (DB-1; inner diameter, 0.25 mm; film thickness, 0.1 µm) was used for the separation.

Phosphatidylethanolamine and sphingolipid analysis by Electrospray Mass Spectrometry. To analyze relative abundance of phosphatidylethanolamine and sphingolipids, parasite lipids were extracted using the Bligh–Dyer approach [49] and examined by electrospray mass spectrometry in the negative ion mode as previously described [50].

Statistics Prism (Graphpad, San Diego, CA), Sigmaplot 11.0 (Systat Software Inc, San Jose, CA) or Excel were used for statistical analysis. Data are represented as mean ± SEM as indicated. The LC_{50} for toxins was calculated by linear regression of the linear portion of the death curve. Statistical significance was determined either by one-way ANOVA with Tukey post-testing, one-way ANOVA (Brown-Forsythe method) with Dunnett T3 post-testing, or Kruskal-Wallis, as appropriate. $p < 0.05$ was considered to be statistically significant. Graphs were generated in Excel and Photoshop (Adobe, San Jose, CA, USA).

Acknowledgments

The authors would like to thank members of the Keyel and Zhang labs for critical review of the manuscript. We thank the College of Arts and Sciences Microscopy for use of facilities.

Funding

This work was supported by American Heart Association grant 16SDG30200001 and National Institute Of Allergy And Infectious Diseases of the National Institutes of Health grant R21AI156225 to PAK, R01AI31078 to SMB, P30DK056341 and P41GM103422 to the Center of Mass Spectrometry Resource of Washington University School of Medicine, and R01AI139198 to KZ (co-I). CH would like to acknowledge financial awards offered by Study Abroad Competitive Scholarship, Office of International Affairs and Summer Dissertation Research Award, Texas Tech Graduate School. FMK would like to acknowledge support through NIH Grant T32AI007172. The funders had no role in study design, data collection and analysis, decision to publish, or preparation of the manuscript. The content is solely the responsibility of the authors and does not necessarily represent the official views of the funding agencies.

Author Contributions

Conceptualization-CH, KZ, PAK; Formal Analysis-CH, PAK; Funding Acquisition-SMB, KZ, PAK; Investigation-CH, SM, RK, FMK, CF; Methodology-CH, SM, CF, FH, RK, PAK; Project Administration-KZ, PAK; Resources-FMK, FH, SMB, KZ, PAK; Supervision-PAK; Visualization-CH, PAK; Writing-Original Draft Preparation-CH, SM, RK, KZ, PAK; Writing-Review & Editing-CH, SM, RK, FMK, CF, FH, SMB, KZ, PAK

Conflicts of Interest

The authors declare they have no competing conflicts of interest. The funding agencies had no role in the design of the study; in the collection, analysis, or interpretation of data; in the writing of the manuscript; nor in the decision to publish the results.

References

1. Baginski M, Czub J. Amphotericin B and its new derivatives - mode of action. Curr Drug Metab. 2009;10(5):459-69. Epub 2009/08/20. doi: 10.2174/138920009788898019. PubMed PMID: 19689243.

2. Berman J. Current treatment approaches to leishmaniasis. Current opinion in infectious diseases. 2003;16(5):397-401. doi: 10.1097/00001432-200310000-00005. PubMed PMID: 14501991.

3. Coukell AJ, Brogden RN. Liposomal amphotericin B. Therapeutic use in the management of fungal infections and visceral leishmaniasis. Drugs. 1998;55(4):585-612. doi: 10.2165/00003495-199855040-00008. PubMed PMID: 9561346.

4. Das A, Brown MS, Anderson DD, Goldstein JL, Radhakrishnan A. Three pools of plasma membrane cholesterol and their relation to cholesterol homeostasis. eLife. 2014;3:e02882. doi: 10.7554/eLife.02882. PubMed PMID: 24920391; PubMed Central PMCID: PMC4086274.

5. Schoenauer R, Larpin Y, Babiychuk EB, Drucker P, Babiychuk VS, Avota E, et al. Down-regulation of acid sphingomyelinase and neutral sphingomyelinase-2 inversely determines the cellular resistance to plasmalemmal injury by pore-forming toxins. FASEB J. 2019;33(1):275-85. doi: 10.1096/fj.201800033R. PubMed PMID: 29979630.

6. Zhang K, Showalter M, Revollo J, Hsu FF, Turk J, Beverley SM. Sphingolipids are essential for differentiation but not growth in Leishmania. EMBO J. 2003;22(22):6016-26. doi: 10.1093/emboj/cdg584. PubMed PMID: 14609948; PubMed Central PMCID: PMC275442.

7. Zhang K, Beverley SM. Phospholipid and sphingolipid metabolism in Leishmania. Mol Biochem Parasitol. 2010;170(2):55-64. doi: 10.1016/j.molbiopara.2009.12.004. PubMed PMID: 20026359; PubMed Central PMCID: PMC2815228.

8. Sepcic K, Berne S, Rebolj K, Batista U, Plemenitas A, Sentjurc M, et al. Ostreolysin, a pore-forming protein from the oyster mushroom, interacts specifically with membrane cholesterol-rich lipid domains. FEBS Lett. 2004;575(1-3):81-5. doi:

10.1016/j.febslet.2004.07.093. PubMed PMID: 15388337.

9. Yamaji A, Sekizawa Y, Emoto K, Sakuraba H, Inoue K, Kobayashi H, et al. Lysenin, a novel sphingomyelin-specific binding protein. J Biol Chem. 1998;273(9):5300-6. Epub 1998/03/28. doi: 10.1074/jbc.273.9.5300. PubMed PMID: 9478988.

10. Zhang O, Wilson MC, Xu W, Hsu FF, Turk J, Kuhlmann FM, et al. Degradation of host sphingomyelin is essential for Leishmania virulence. PLoS Pathog. 2009;5(12):e1000692. doi: 10.1371/journal.ppat.1000692. PubMed PMID: 20011126; PubMed Central PMCID: PMC2784226.

11. Thapa R, Ray S, Keyel PA. Interaction of Macrophages and Cholesterol-Dependent Cytolysins: The Impact on Immune Response and Cellular Survival. Toxins (Basel). 2020;12(9). doi: 10.3390/toxins12090531. PubMed PMID: 32825096.

12. Savinov SN, Heuck AP. Interaction of Cholesterol with Perfringolysin O: What Have We Learned from Functional Analysis? Toxins (Basel). 2017;9(12):381. Epub 2017/11/24. doi: 10.3390/toxins9120381. PubMed PMID: 29168745; PubMed Central PMCID: PMCPMC5744101.

13. Ray S, Thapa R, Keyel PA. Multiple Parameters Beyond Lipid Binding Affinity Drive Cytotoxicity of Cholesterol-Dependent Cytolysins. Toxins (Basel). 2018;11(1). doi: 10.3390/toxins11010001. PubMed PMID: 30577571.

14. Farrand AJ, Hotze EM, Sato TK, Wade KR, Wimley WC, Johnson AE, et al. The Cholesterol-dependent Cytolysin Membrane-binding Interface Discriminates Lipid Environments of Cholesterol to Support beta-Barrel Pore Insertion. J Biol Chem. 2015;290(29):17733-44. doi: 10.1074/jbc.M115.656769. PubMed PMID: 26032415; PubMed Central PMCID: PMC4505022.

15. Hotze EM, Heuck AP, Czajkowsky DM, Shao Z, Johnson AE, Tweten RK. Monomer-monomer interactions drive the prepore to pore conversion of a beta-barrel-forming cholesterol-dependent cytolysin. J Biol Chem. 2002;277(13):11597-605. doi: 10.1074/jbc.M111039200. PubMed PMID: 11799121.

16. Johnson BB, Moe PC, Wang D, Rossi K, Trigatti BL, Heuck AP. Modifications in perfringolysin O domain 4 alter the cholesterol concentration threshold required for binding. Biochemistry. 2012;51(16):3373-82. doi: 10.1021/bi3003132. PubMed PMID: 22482748.

17. Magassa N, Chandrasekaran S, Caparon MG. Streptococcus pyogenes cytolysin-mediated translocation does not require pore formation by streptolysin O. EMBO Rep. 2010;11(5):400-5. Epub 2010/03/27. doi: embor201037 [pii] 10.1038/embor.2010.37. PubMed PMID: 20339385; PubMed Central PMCID: PMC2868537.

18. Mozola CC, Caparon MG. Dual modes of membrane binding direct pore formation by Streptolysin O. Mol Microbiol. 2015;97(6):1036-50. doi: 10.1111/mmi.13085. PubMed PMID: 26059530.

19. Romero M, Keyel M, Shi G, Bhattacharjee P, Roth R, Heuser JE, et al. Intrinsic repair protects cells from pore-forming toxins by microvesicle shedding. Cell Death Differ. 2017;24(5):798-808. doi: 10.1038/cdd.2017.11. PubMed PMID: 28186501.

20. Kuhlmann FM, Key P, Hickerson S, Turck J, Hsu F-f, Beverley SM. Inositol Phosphorlyceramide Synthase null Leishmania major (Δipcs-) are viable and virulent in animal infections where salvage of host sphingomyelin predominates. biorxiv. 2022. Epub 6/15/22. doi: 10.1101/2022.06.14.496188.

21. Armitage EG, Alqaisi AQI, Godzien J, Pena I, Mbekeani AJ, Alonso-Herranz V, et al. Complex Interplay between Sphingolipid and Sterol Metabolism Revealed by Perturbations to the Leishmania Metabolome Caused by Miltefosine. Antimicrob Agents Chemother. 2018;62(5). Epub 2018/02/22. doi: 10.1128/AAC.02095-17. PubMed PMID: 29463533; PubMed Central PMCID: PMCPMC5923112.

22. Mukherjee S, Xu W, Hsu FF, Patel J, Huang J, Zhang K. Sterol methyltransferase is required for optimal mitochondrial function and virulence in Leishmania major. Mol Microbiol. 2019;111(1):65-81. doi: 10.1111/mmi.14139. PubMed PMID: 30260041; PubMed Central PMCID: PMC6351164.

23. Shewell LK, Day CJ, Jen FE, Haselhorst T, Atack JM, Reijneveld JF, et al. All major cholesterol-dependent cytolysins use glycans as cellular receptors. Science advances. 2020;6(21):eaaz4926. Epub 2020/06/05. doi: 10.1126/sciadv.aaz4926. PubMed PMID: 32494740; PubMed Central PMCID: PMCPMC7244308.

24. Zhang K, Pompey JM, Hsu FF, Key P, Bandhuvula P, Saba JD, et al. Redirection of sphingolipid metabolism toward de novo synthesis of ethanolamine in Leishmania. EMBO J. 2007;26(4):1094-104. doi: 10.1038/sj.emboj.7601565. PubMed PMID: 17290222; PubMed Central PMCID: PMC1852826.

25. Seifert K, Croft SL. In vitro and in vivo interactions between miltefosine and other antileishmanial drugs. Antimicrob Agents Chemother. 2006;50(1):73-9. Epub 2005/12/27. doi: 10.1128/AAC.50.1.73-79.2006. PubMed PMID: 16377670; PubMed Central PMCID: PMCPMC1346816.

26. Nelson LD, Johnson AE, London E. How interaction of perfringolysin O with membranes is controlled by sterol structure, lipid structure, and physiological low pH: insights into the origin of perfringolysin O-lipid raft interaction. J Biol Chem. 2008;283(8):4632-42. doi: 10.1074/jbc.M709483200. PubMed PMID: 18089559.

27. Brittingham A, Morrison CJ, McMaster WR, McGwire BS, Chang KP, Mosser DM. Role of the Leishmania surface protease gp63 in complement fixation, cell adhesion, and resistance to complement-mediated lysis. J Immunol. 1995;155(6):3102-11. Epub 1995/09/15. PubMed PMID: 7673725.

28. Endapally S, Frias D, Grzemska M, Gay A, Tomchick DR, Radhakrishnan A. Molecular Discrimination between Two Conformations of Sphingomyelin in Plasma Membranes. Cell. 2019. doi: 10.1016/j.cell.2018.12.042. PubMed PMID: 30712872.

29. Giddings KS, Johnson AE, Tweten RK. Redefining cholesterol's role in the mechanism of the cholesterol-dependent cytolysins. Proc Natl Acad Sci U S A. 2003;100(20):11315-20. PubMed PMID: 14500900.

30. Rodal SK, Skretting G, Garred O, Vilhardt F, van Deurs B, Sandvig K. Extraction of cholesterol with methyl-beta-cyclodextrin perturbs formation of clathrin-coated endocytic vesicles. Mol Biol Cell. 1999;10(4):961-74. PubMed PMID: 10198050.

31. Sen S, Roy K, Mukherjee S, Mukhopadhyay R, Roy S. Restoration of IFNgammaR subunit assembly, IFNgamma signaling and parasite clearance in Leishmania donovani infected macrophages: role of membrane cholesterol. PLoS Pathog. 2011;7(9):e1002229. doi: 10.1371/journal.ppat.1002229. PubMed PMID: 21931549; PubMed Central PMCID: PMC3169561.

32. Subramaniam PS, Johnson HM. Lipid microdomains are required sites for the selective endocytosis and nuclear translocation of IFN-gamma, its receptor chain IFN-gamma receptor-1, and the phosphorylation and nuclear translocation of STAT1alpha. J Immunol. 2002;169(4):1959-69. PubMed PMID: 12165521.

33. Lange Y, Tabei SM, Ye J, Steck TL. Stability and stoichiometry of bilayer phospholipid-cholesterol complexes: relationship to cellular sterol distribution and homeostasis. Biochemistry. 2013;52(40):6950-9. Epub 2013/09/05. doi: 10.1021/bi400862q. PubMed PMID: 24000774; PubMed Central PMCID: PMCPMC3859718.

34. Henriques C, Atella GC, Bonilha VL, de Souza W. Biochemical analysis of proteins and lipids found in parasitophorous vacuoles containing Leishmania amazonensis. Parasitol Res. 2003;89(2):123-33. Epub 2002/12/19. doi: 10.1007/s00436-002-0728-y. PubMed PMID: 12489012.

35. Moitra S, Basu S, Pawlowic M, Hsu FF, Zhang K. De Novo Synthesis of Phosphatidylcholine Is Essential for the Promastigote But Not Amastigote Stage in Leishmania major. Frontiers in cellular and infection microbiology. 2021;11:647870. Epub 2021/03/30. doi: 10.3389/fcimb.2021.647870. PubMed PMID: 33777852; PubMed Central PMCID: PMCPMC7996062.

36. Winter G, Fuchs M, McConville MJ, Stierhof YD, Overath P. Surface antigens of

Leishmania mexicana amastigotes: characterization of glycoinositol phospholipids and a macrophage-derived glycosphingolipid. J Cell Sci. 1994;107 (Pt 9):2471-82. Epub 1994/09/01. PubMed PMID: 7844164.

37. Zhang K, Hsu FF, Scott DA, Docampo R, Turk J, Beverley SM. Leishmania salvage and remodelling of host sphingolipids in amastigote survival and acidocalcisome biogenesis. Mol Microbiol. 2005;55(5):1566-78. doi: 10.1111/j.1365-2958.2005.04493.x. PubMed PMID: 15720561; PubMed Central PMCID: PMC3803142.

38. Tam C, Idone V, Devlin C, Fernandes MC, Flannery A, He X, et al. Exocytosis of acid sphingomyelinase by wounded cells promotes endocytosis and plasma membrane repair. J Cell Biol. 2010;189(6):1027-38. doi: 10.1083/jcb.201003053. PubMed PMID: 20530211; PubMed Central PMCID: PMC2886342.

39. Puentes SM, Sacks DL, da Silva RP, Joiner KA. Complement binding by two developmental stages of Leishmania major promastigotes varying in expression of a surface lipophosphoglycan. J Exp Med. 1988;167(3):887-902. Epub 1988/03/01. doi: 10.1084/jem.167.3.887. PubMed PMID: 3280727; PubMed Central PMCID: PMCPMC2188887.

40. Zitzer A, Bittman R, Verbicky CA, Erukulla RK, Bhakdi S, Weis S, et al. Coupling of cholesterol and cone-shaped lipids in bilayers augments membrane permeabilization by the cholesterol-specific toxins streptolysin O and Vibrio cholerae cytolysin. J Biol Chem. 2001;276(18):14628-33. PubMed PMID: 11279036.

41. Ogretmen B. Sphingolipid metabolism in cancer signalling and therapy. Nat Rev Cancer. 2018;18(1):33-50. Epub 2017/11/18. doi: 10.1038/nrc.2017.96. PubMed PMID: 29147025; PubMed Central PMCID: PMCPMC5818153.

42. Babiychuk EB, Monastyrskaya K, Potez S, Draeger A. Intracellular Ca(2+) operates a switch between repair and lysis of streptolysin O-perforated cells. Cell Death Differ. 2009;16(8):1126-34. PubMed PMID: 19325569.

43. Keyel PA, Roth R, Yokoyama WM, Heuser JE, Salter RD. Reduction of streptolysin O

(SLO) pore-forming activity enhances inflammasome activation. Toxins (Basel). 2013;5(6):1105-18. Epub 2013/06/08. doi: 10.3390/toxins5061105. PubMed PMID: 23744055; PubMed Central PMCID: PMC3717772.

44. Farrand AJ, LaChapelle S, Hotze EM, Johnson AE, Tweten RK. Only two amino acids are essential for cytolytic toxin recognition of cholesterol at the membrane surface. Proc Natl Acad Sci U S A. 2010;107(9):4341-6. PubMed PMID: 20145114.

45. Keyel PA, Heid ME, Watkins SC, Salter RD. Visualization of bacterial toxin induced responses using live cell fluorescence microscopy. J Vis Exp. 2012;(68):e4227. Epub 2012/10/12. doi: 4227 [pii]
10.3791/4227. PubMed PMID: 23052609.

46. Zhang O, Xu W, Balakrishna Pillai A, Zhang K. Developmentally regulated sphingolipid degradation in Leishmania major. PLoS One. 2012;7(1):e31059. doi: 10.1371/journal.pone.0031059. PubMed PMID: 22299050; PubMed Central PMCID: PMC3267774.

47. Keyel PA, Loultcheva L, Roth R, Salter RD, Watkins SC, Yokoyama WM, et al. Streptolysin O clearance through sequestration into blebs that bud passively from the plasma membrane. J Cell Sci. 2011;124(Pt 14):2414-23. Epub 2011/06/23. doi: jcs.076182 [pii] 10.1242/jcs.076182. PubMed PMID: 21693578.

48. Folch J, Lees M, Sloane Stanley GH. A simple method for the isolation and purification of total lipides from animal tissues. J Biol Chem. 1957;226(1):497-509. Epub 1957/05/01. PubMed PMID: 13428781.

49. Bligh EG, Dyer WJ. A rapid method of total lipid extraction and purification. Can J Biochem Physiol. 1959;37(8):911-7. Epub 1959/08/01. doi: 10.1139/o59-099. PubMed PMID: 13671378.

50. Pawlowic MC, Hsu FF, Moitra S, Biyani N, Zhang K. Plasmenylethanolamine synthesis in Leishmania major. Mol Microbiol. 2016;101(2):238-49. doi: 10.1111/mmi.13387. PubMed

PMID: 27062077; PubMed Central PMCID: PMC4935589.

Figure Legends

Figure 1. CDCs bind to *Leishmania major* promastigotes independently of sphingolipids. (A, B) Wild type (WT), *spt2*$^{-}$, and *spt2*$^{-}$/+SPT2, or (C, D) WT, *ipcs*$^{-}$, and *ipcs*$^{-}$/+IPCS *L. major* promastigotes were challenged with the indicated mass of (A, C) monomer-locked SLO (SLO ML) conjugated to Cy5 or (B, D) monomer-locked PFO (PFO ML) conjugated to Cy5 at 37ºC for 30 min and analyzed by flow cytometry. (E) Total sterols from DMSO treated WT, *spt2*$^{-}$, and *spt2*$^{-}$/+SPT2, or WT treated with 10 μM myriocin *L. major* promastigotes were extracted, derivatized and analyzed by GC-MS. (F) HeLa cells or WT, *spt2*$^{-}$, or *spt2*$^{-}$/+SPT2 *L. major* promastigotes were challenged with SLO ML conjugated to Cy5 and analyzed by flow cytometry. Median Fluorescence Intensity x10 (MFI) of Cy5 fluorescence gated on live cells is shown. Graphs display the mean ± SEM of 3 independent experiments. * $p < 0.05$

Figure 2. IPC protects *L. major* promastigotes from lysis by CDCs. (A, B) Wild type (WT), *spt2*$^{-}$, and *spt2*$^{-}$/+SPT2, or (C, D) WT, *ipcs*$^{-}$, and *ipcs*$^{-}$/+IPCS *L. major* promastigotes were challenged with (A, C) SLO or (B, D) PFO at the indicated concentrations for 30 min at 37°C and PI uptake measured by flow cytometry. (E-G) The LC_{50} was calculated as described in the methods after challenging the indicated genotypes of *L. major* with 31-4000 HU/mL or HeLa cells with 32-2000 HU/mL of SLO or PFO for 30 min (E, F) or 5 min (F, G) and measuring PI uptake by flow cytometry. (A-D) Graphs display the mean ±SEM of at least 3 independent experiments. The dashed line indicates the highest concentration used. Points on this line had a LC_{50} value ≥64,000 HU/mL. (E-G) Graphs display individual data points and median from at least 3 independent experiments. Statistical significance ($p<0.05$) was assessed by post-hoc testing between groups. Groups sharing the same letter were not statistically different.

Figure 3. Transition to stationary phase does not alter CDC sensitivity of *spt2*$^{-}$ *L. major* promastigotes. *spt2*$^{-}$ *L. major* promastigotes in each day of stationary phase were challenged

with (A) PFO, or (B, C) SLO for (A-C) 30 min or (C) 5 min at 37°C. PI uptake was analyzed by flow cytometry and LC_{50} calculated as described in the methods. Stationary phase d1, d2 and d3 represents 48, 72 and 96 hours post log phase. Graphs show individual data points and the median from at least 3 independent experiments. * $p < 0.05$

Figure 4. Myriocin treatment of *L. major* promastigotes suggests ceramide helps shield ergosterol. (A, B) Wild type (WT), *spt2*$^{-}$, spt2^{-}/+SPT2, *ipcs*$^{-}$ and *ipcs*$^{-}$/+IPCS *L. major* promastigotes grown in either 10 μM Myriocin or DMSO supplemented M199 media were challenged with (A) SLO or (B) PFO for 30 min at 37°C. (C, D) WT, *iscl*$^{-}$, *iscl*$^{-}$/+ISCL, *ipcs*$^{-}$ and *ipcs*$^{-}$/+IPCS *L. major* promastigotes grown in either 10 μM Myriocin or DMSO supplemented M199 media were challenged with (C) SLO or (D) PFO for 30 min at 37°C. PI uptake was analyzed by flow cytometry and LC_{50} calculated as described in the methods. WT, *ipcs*$^{-}$ and *ipcs*$^{-}$/+IPCS represent distinct assays in each panel. Graphs display medians from at least 3 independent experiments. The dashed line indicates the highest concentration used. Points on this line had a LC_{50} value ≥4000 HU/mL. Statistical significance ($p<0.05$) was assessed by post-hoc testing between groups. Groups sharing the same letter were not statistically different.

Figure 5. The CDC L3 loop controls CDC cytotoxicity against *L. major* promastigotes. (A, B) Wild type (WT), *spt2*$^{-}$, and *spt2*$^{-}$/+SPT2 or (C, D) WT, *ipcs*$^{-}$, and *ipcs*$^{-}$/+IPCS *Leishmania major* promastigotes were challenged with (A, C) PFO WT, PFO D434K, (B, D) SLO WT, or SLO S505D at the indicated concentrations for 30 min at 37°C. PI uptake was analyzed by flow cytometry and (E) LC_{50} calculated as described in the methods. (A-D) Graphs display the mean ±SEM of at least 3 independent experiments. (E) Graph displays individual data points and median from at least 3 independent experiments. The dashed line indicates the highest concentration used. Points on this line had a LC_{50} value ≥64,000 HU/mL. Both *spt2*$^{-}$ and *ipcs*$^{-}$

were statistically significant compared to WT or *ipcs*$^{-}$/+IPCS by 2-way ANOVA. Statistical significance ($p<0.05$) was assessed by post-hoc testing between groups. Within the same genotype, groups sharing the same letter were not statistically different.

Figure 6. Ceramide protects *L. major* promastigotes from amphotericin B. (A) Untreated wild type (WT), *spt2*$^{-}$, and *spt2*$^{-}$/+SPT2, *ipcs*$^{-}$,*ipcs*$^{-}$/+IPCS or 10 μM myriocin-treated WT *L. major* promastigotes were challenged with the indicated concentration of amphotericin B and growth determined relative to untreated WT. The (B) EC_{50} and (C) EC_{25} were calculated by logistic regression. Graphs display the mean ± SEM of 3 independent experiments. Statistical significance was determined by one-way ANOVA. Statistical significance ($p<0.05$) was assessed by post-hoc testing between groups. Groups sharing the same letter were not statistically different.

Figure 7. Cytotoxicity of CDCs towards *L. major* promastigotes is dependent on the presence of IPC. CDCs can bind to ergosterol in the membrane of *L. major* promastigotes regardless of sphingolipids. In the absence of IPC and ceramide, both SLO and PFO form lytic pores in the membrane. Elimination of IPC, but not ceramide, favors SLO pore formation, but reduced PFO pore formation. In the presence of ceramide and IPC, only SLO can still form pores at high doses (Toxin+++). At lower toxin doses (Toxin+), neither toxin can form pores in the membrane.

Supplemental Figure Legends

Supplementary Figure S1. Gating strategy for *Leishmania major* promastigotes. Total *Leishmania major* promastigotes are gated on R1 gate for SSC-H and FSC-H. *L. major* promastigotes are then gated for single cells (R2) using FSC-A and FSC-H. From R2, *L. major* promastigotes are gated for fluorescence intensity of propidium iodide (PI) for dead cells and live cells.

Supplementary Figure S2. Pore-formation, glycan- and sterol- binding determinants are all required for cytotoxicity in *Leishmania major* promastigotes. (A, B) Wild type (WT), *spt2*$^{-}$, and *spt2*$^{-}$/+SPT2, or (C, D) WT, *ipcs*$^{-}$, and *ipcs*$^{-}$/+IPCS *L. major* promastigotes were challenged with (A) monomer-locked SLO (SLO ML), (B) monomer-locked PFO (PFO ML), (A, C) SLO or (B, D) PFO at the indicated concentrations for 30 min at 37°C and PI uptake measured by flow cytometry. (E) Hela cells were challenged with SLO WT or PFO WT at the indicated concentrations for 30 min at 37°C and PI uptake measured by flow cytometry. (F, G) WT, *smt*$^{-}$, and *smt*$^{-}$/+SMT, or *spt2*$^{-}$ *L. major* promastigotes were challenged with (F) SLO ML conjugated to Cy5 or (G) SLO at the indicated concentrations for 30 min at 37°C and PI uptake measured by flow cytometry. (H) *spt2*$^{-}$ and (I) *ipcs*$^{-}$ *L. major* promastigotes were challenged with SLO (WT), SLO Q476N or SLO ΔCRM at the indicated concentrations for 30 min at 37°C. PI uptake was analyzed by flow cytometry. Graphs display mean ± SEM of 3 independent experiments.

Supplementary Figure S3. Sphingolipid-deficient mutants of *L. major* are susceptible to CDCs. (A, B) WT, *spt2*$^{-}$, and *spt2*$^{-}$/+SPT2, or (C, D) WT, *ipcs*$^{-}$, and *ipcs*$^{-}$/+IPCS *L. major* promastigotes were challenged with (A, C) SLO or (B, D) PFO at the indicated concentrations for 5 min at 37°C. PI uptake was measured by flow cytometry. Graphs display mean ± SEM of at least 3 independent experiments.

Supplementary Figure S4. Sensitivity of *spt2*⁻ *L. major* promastigotes to CDCs remains the same across three consecutive days of stationary phase. Stationary phase wild type (WT), *spt2*⁻ and *spt2*⁻/+SPT2 *L. major* promastigotes were challenged with (A-C) PFO for 30 min (D-F) SLO for 30 min or (G-I) SLO for 5 min at 37°C at indicated concentrations. PI uptake was analyzed by flow cytometry. Stationary phase (A, D, G) d1, (B, E, H) d2 and (C, F, I) d3 represents 48, 72 and 96 hours post log phase. Graphs display mean ± SEM of 3 independent experiments.

Supplementary Figure S5. Chemical blockade of SPT enhances CDC cytotoxicity against *L. major* promastigotes. (A, B) Wild type (WT), *spt2*⁻, *spt2*⁻/+SPT2, *ipcs*⁻ and *ipcs*⁻/+IPCS *L. major* promastigotes were grown in either 10 μM Myriocin or DMSO supplemented M199 media, and challenged with (A) SLO and (B) PFO for 30 min. PI uptake was measured by flow cytometry and specific lysis determined. (C, D) WT, *iscl*⁻, *iscl*⁻/+ISCL, *ipcs*⁻ and *ipcs*⁻/+IPCS *L. major* promastigotes were grown in either 10 μM Myriocin or DMSO supplemented M199 media, and challenged with (C) SLO and (D) PFO for 30 min at 37°C. PI uptake was measured by flow cytometry and specific lysis determined. Graphs display mean ±SEM of (A, B) 3, (C), 4, or (D) 2 independent experiments.

Figure 1

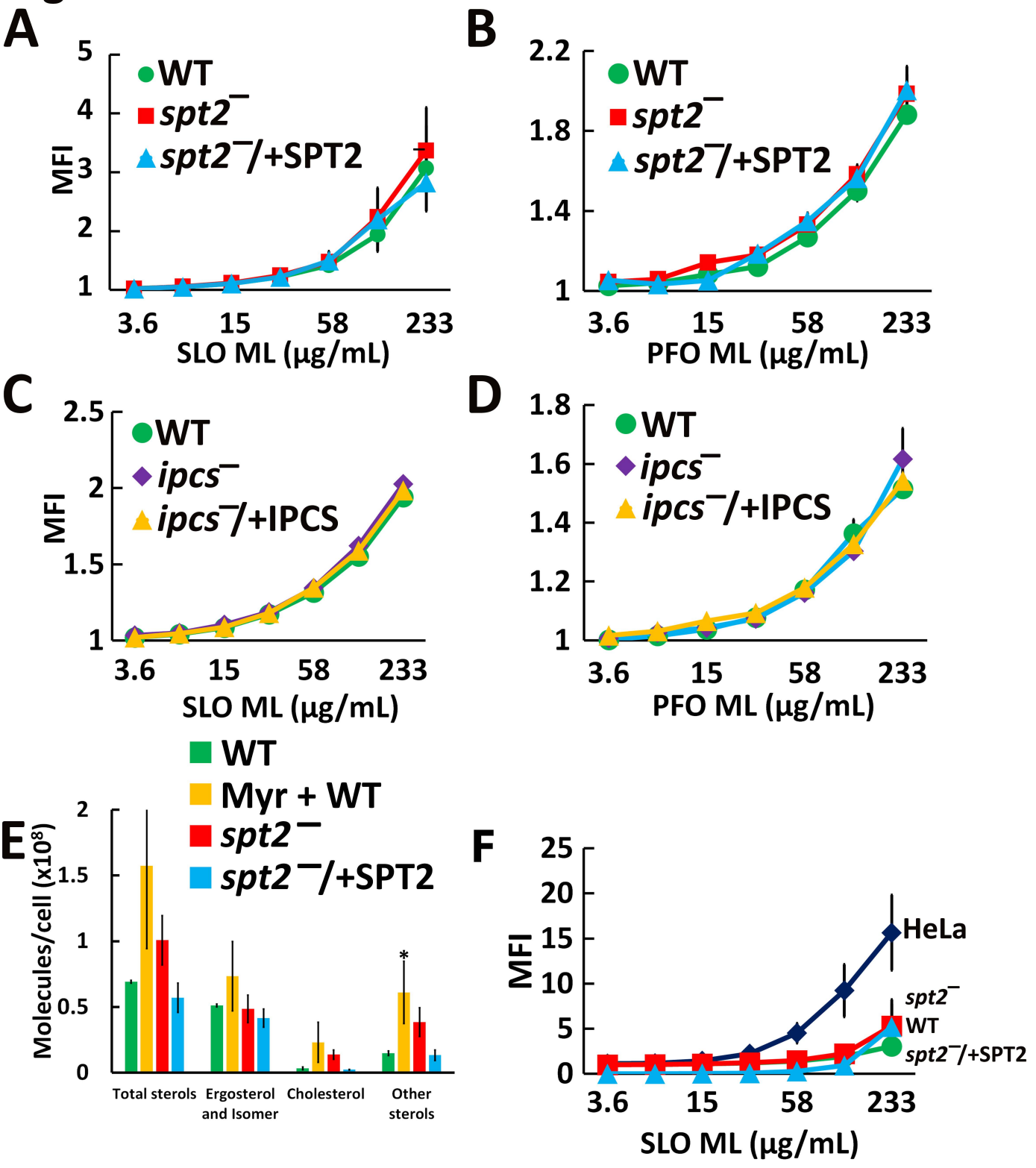
A
WT
spt2⁻
spt2⁻/+SPT2
MFI
SLO ML (µg/mL)
3.6
15
58
233
B
PFO ML (µg/mL)
C
ipcs⁻
ipcs⁻/+IPCS
D
E
Myr + WT
Molecules/cell (x10⁸)
Total sterols
Ergosterol and Isomer
Cholesterol
Other sterols
F
HeLa

Figure 2

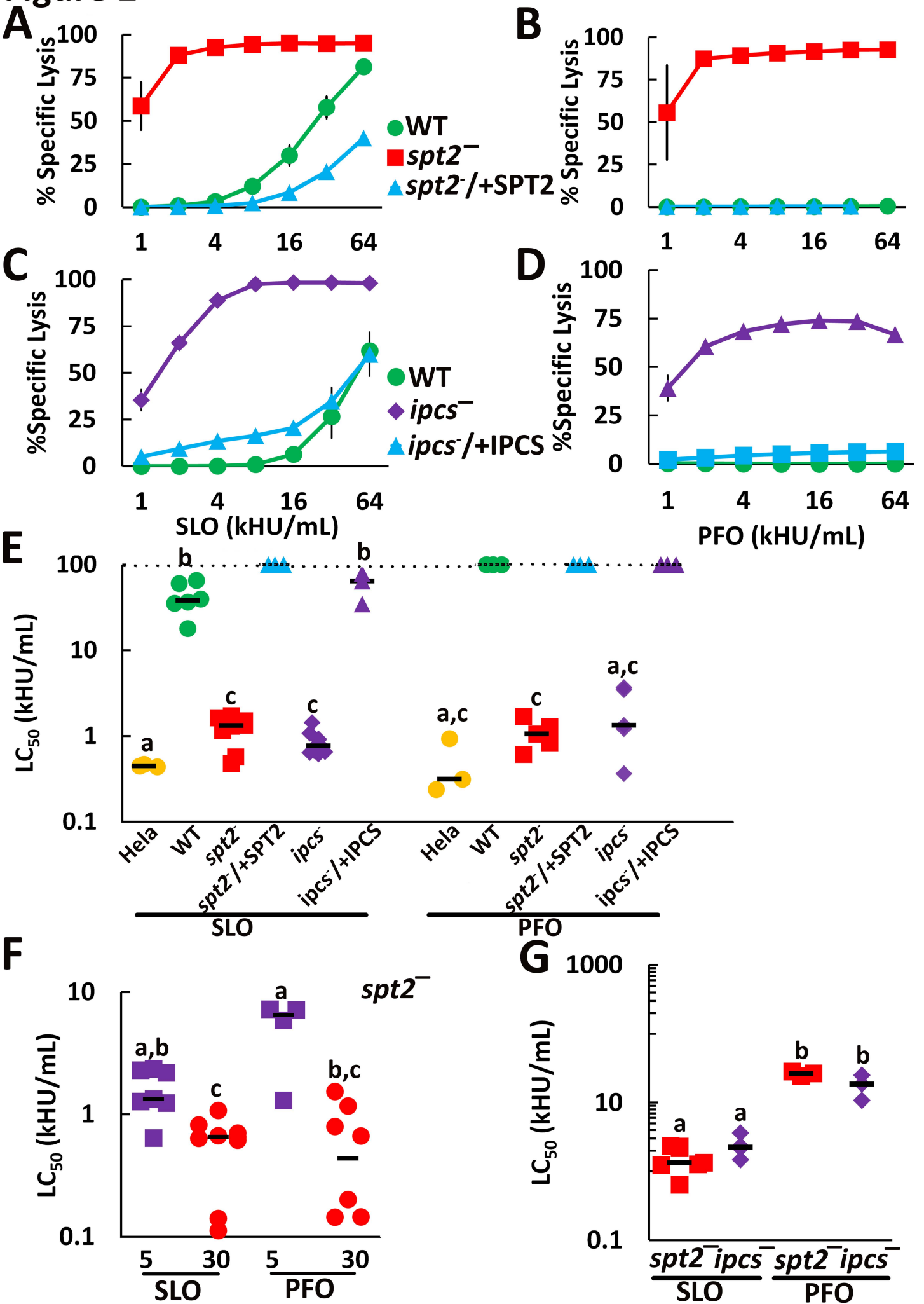

Figure 3

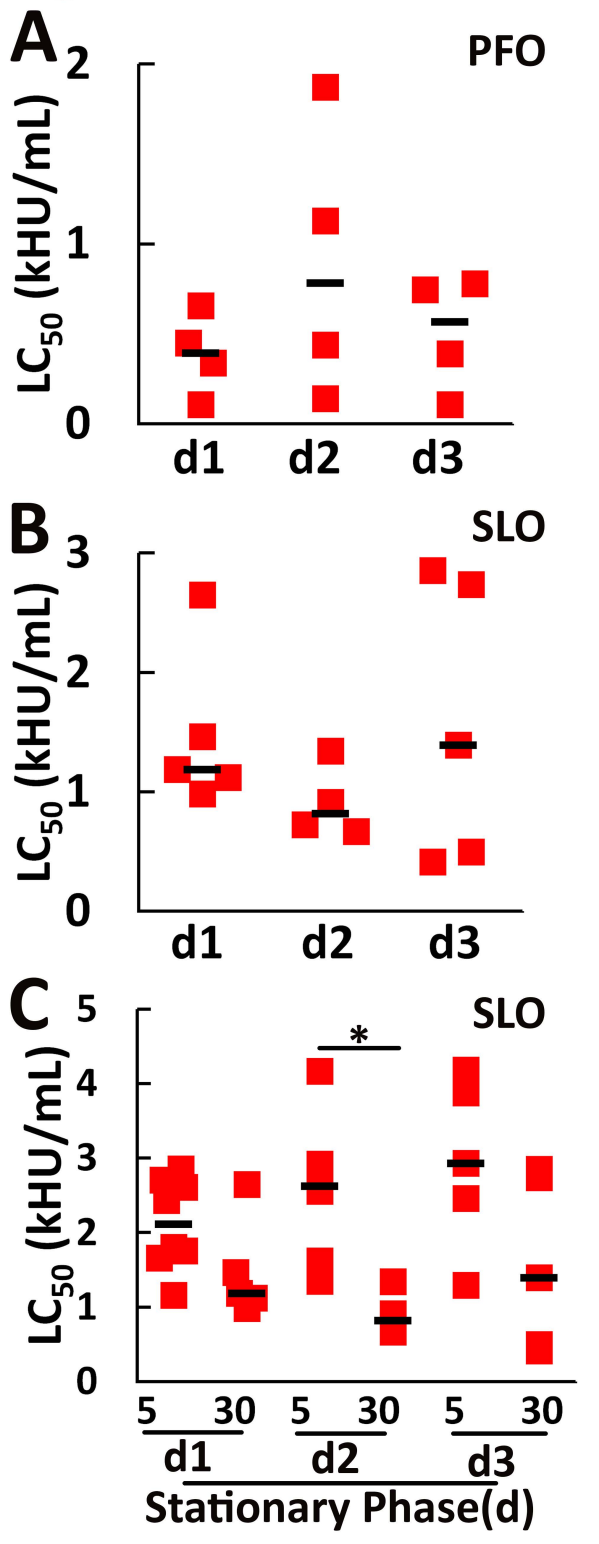
A
PFO
LC50 (kHU/mL)
0
1
2
d1
d2
d3
B
SLO
LC50 (kHU/mL)
0
1
2
3
d1
d2
d3
C
SLO
*
LC50 (kHU/mL)
0
1
2
3
4
5
5
30
5
30
5
30
d1
d2
d3
Stationary Phase(d)

Figure 4

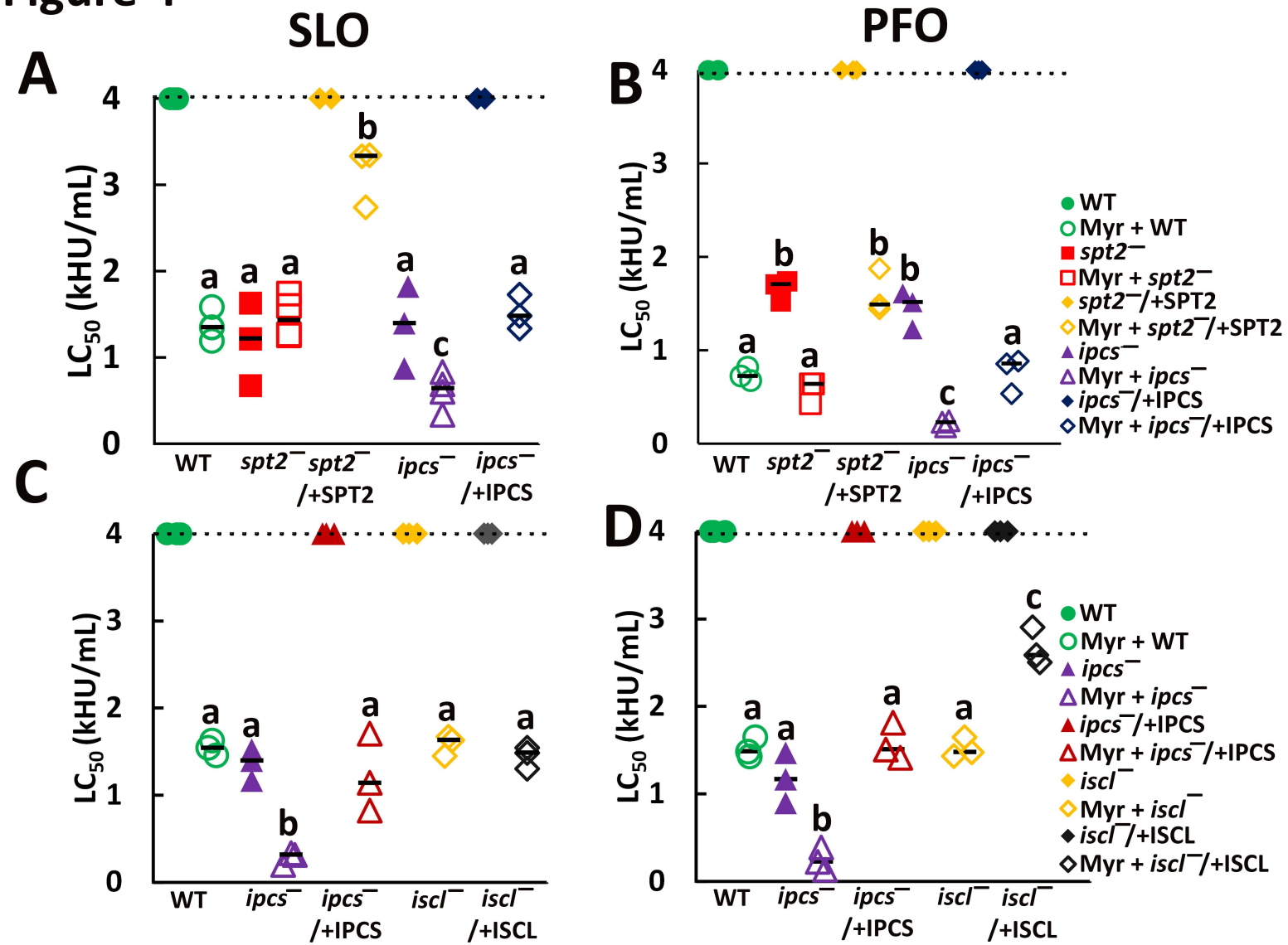
SLO
PFO
A
B
C
D
LC50 (kHU/mL)
0
1
2
3
4
WT
spt2−
spt2− /+SPT2
ipcs−
ipcs− /+IPCS
iscl−
iscl− /+ISCL
a
b
c
WT
Myr + WT
spt2−
Myr + spt2−
spt2−/+SPT2
Myr + spt2−/+SPT2
ipcs−
Myr + ipcs−
ipcs−/+IPCS
Myr + ipcs−/+IPCS
iscl−
Myr + iscl−
iscl−/+ISCL
Myr + iscl−/+ISCL

Figure 5

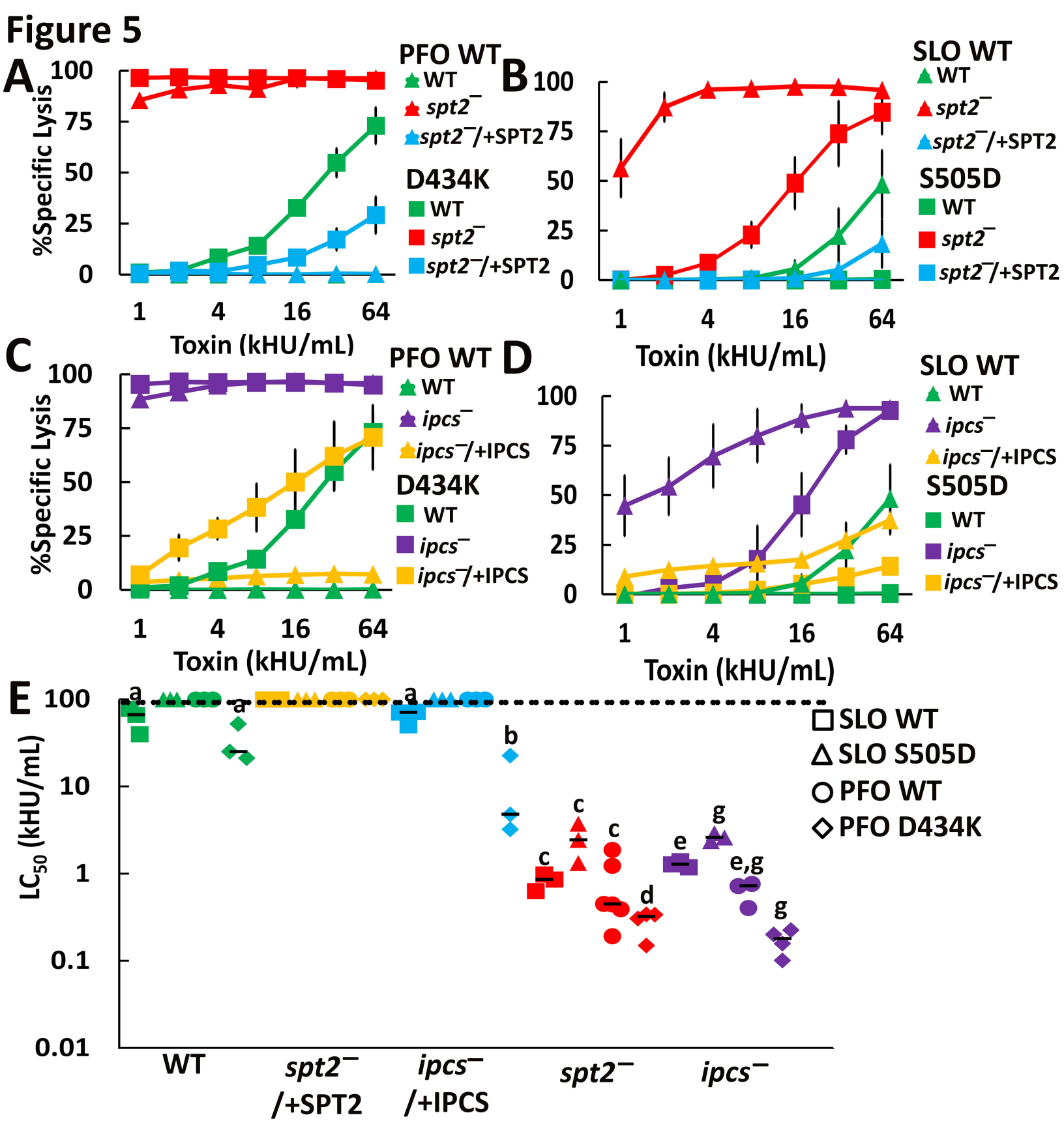
A
%Specific Lysis
100
75
50
25
0
1
4
16
64
Toxin (kHU/mL)
PFO WT
WT
spt2⁻
spt2⁻/+SPT2
D434K
WT
spt2⁻
spt2⁻/+SPT2
B
SLO WT
WT
spt2⁻
spt2⁻/+SPT2
S505D
WT
spt2⁻
spt2⁻/+SPT2
C
%Specific Lysis
PFO WT
WT
ipcs⁻
ipcs⁻/+IPCS
D434K
WT
ipcs⁻
ipcs⁻/+IPCS
D
SLO WT
WT
ipcs⁻
ipcs⁻/+IPCS
S505D
WT
ipcs⁻
ipcs⁻/+IPCS
E
LC50 (kHU/mL)
100
10
1
0.1
0.01
a
a
a
b
c
c
c
d
e
g
e,g
g
SLO WT
SLO S505D
PFO WT
PFO D434K
WT
spt2⁻ /+SPT2
ipcs⁻ /+IPCS
spt2⁻
ipcs⁻

Figure 6

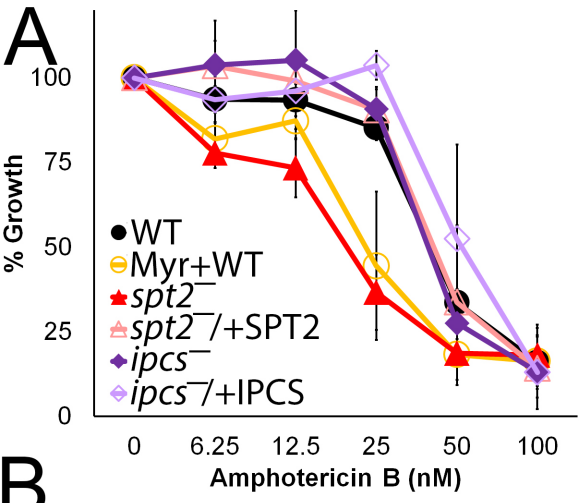
A
100
75
50
25
0
% Growth
WT
Myr+WT
spt2⁻
spt2⁻/+SPT2
ipcs⁻
ipcs⁻/+IPCS
0
6.25
12.5
25
50
100
Amphotericin B (nM)

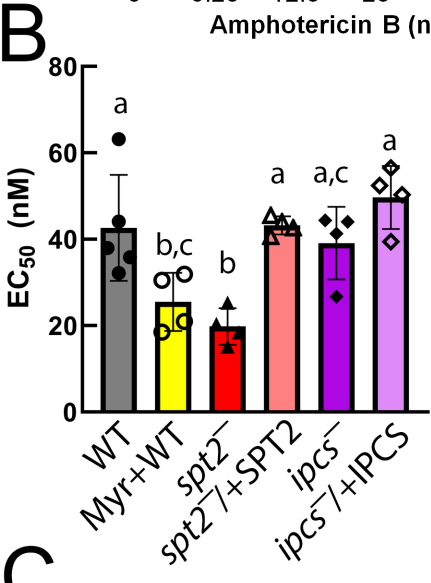
B
80
60
40
20
0
EC50 (nM)
a
b,c
b
a
a,c
a
WT
Myr+WT
spt2⁻
spt2⁻/+SPT2
ipcs⁻
ipcs⁻/+IPCS

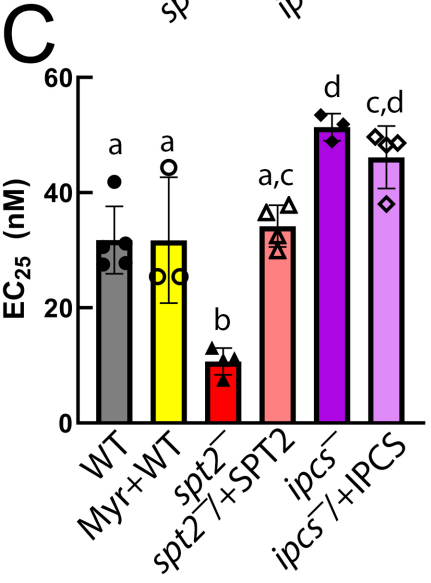
C
60
40
20
0
EC25 (nM)
a
a
b
a,c
d
c,d
WT
Myr+WT
spt2⁻
spt2⁻/+SPT2
ipcs⁻
ipcs⁻/+IPCS

Figure 7

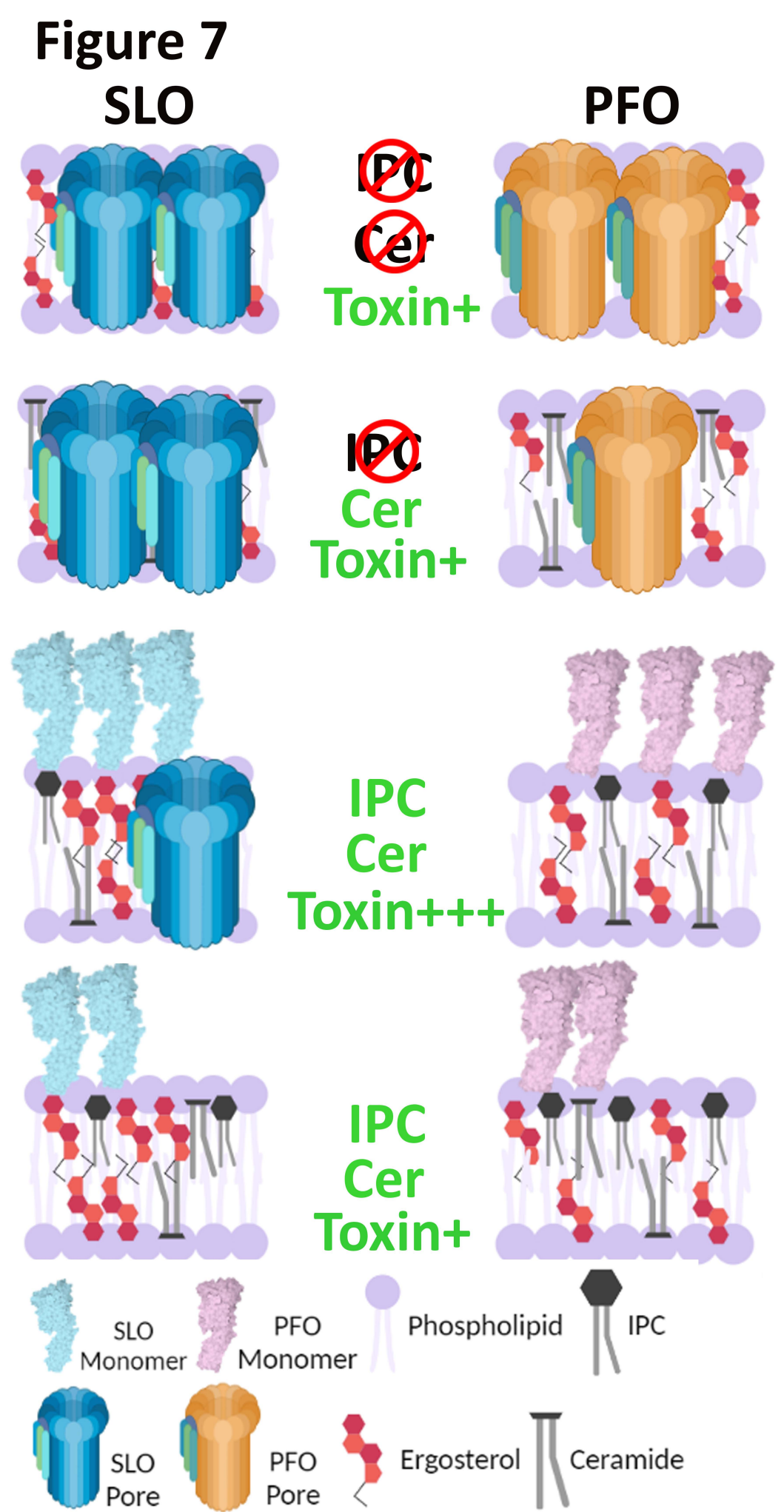
SLO
PFO
IPC
Cer
Toxin+
IPC
Cer
Toxin+
IPC
Cer
Toxin+++
IPC
Cer
Toxin+
SLO Monomer
PFO Monomer
Phospholipid
IPC
SLO Pore
PFO Pore
Ergosterol
Ceramide